

## Phase transition in warm nuclear matter

Guo Hua

*Department of Technical Physics and MOE Key Laboratory of Heavy Ion Physics, Peking University,  
Beijing 100871, People's Republic of China*

Liu Bo

*Institute of High Energy Physics, Chinese Academy of Sciences, Beijing 10039, People's Republic of China*

M. Di Toro

*Laboratori Nazionali del Sud, Via S. Sofia 44, I-95123 Catania, Italy*

(Received 7 April 2000; published 14 August 2000)

A density-dependent relativistic mean field (DRMF) theory is extended to that at finite temperature and density, and the liquid-gas phase transition of warm nuclear matter is investigated. Our results are compared with those obtained from the Walecka's mean field theory. The critical values of temperature, density, and pressure are calculated by the DRMF. The obtained critical temperature is  $T_c = 12.66$  MeV by using the parameter set A, which is in accord with recent experimental observation.

PACS number(s): 21.65.+f, 05.70.Fh, 21.30.Fe, 25.75.-q

### I. INTRODUCTION

There has been considerable interest in heavy-ion collisions which could offer the possibility of producing warm and dilute matter. The liquid-gas transition may take place in warm and dilute matter. Therefore, the study of the liquid-gas phase transition has attracted much attention [1].

With the nonrelativistic theory [2–5], a liquid-gas phase transition was studied and the critical temperature was estimated to be 15–20 MeV. It had also been suggested that liquid-gas mixture exists at very low temperatures ( $\leq 10$  MeV) in the crusts of neutron star in supernovas [6]. Recent experimental results for warm and dilute nuclear matter produced in heavy-ion collision support a small liquid-gas phase region and a low critical temperature  $T_c \approx 13.1 \pm 0.6$  MeV [7].

It is well known that the Walecka's mean field theory has been very successful in describing the properties of nuclear matter and finite nuclei [8]. With the parameters normally fitting to the equilibrium properties of symmetric nuclear matter, the critical temperature given by the Walecka model is  $T_c \approx 18.3$  MeV [8], and reduces to  $T_c \approx 14.2$  MeV [9] if the nonlinear terms are included, while the derivative scalar coupling (DSC) model leads to the low critical temperature,  $T_c = 16.5, 15.5,$  and  $13.6$  MeV for the ZM, ZM2, and ZM3 models, respectively [10]. With the replacement of the nuclear ground-state Green's function by the finite-temperature Green's function, the Dirac-Brückner-Hartree-Fock (DBHF) approach was applied to nuclear matter at finite temperature, and the critical temperature was extracted to be  $T_c = 15.0$  MeV [11]. It was also pointed out that a very low critical temperature,  $T_c \sim 8-9$  MeV, was obtained by relativistic Dirac-Brückner (DB) calculation [12]. However, recent investigation has shown that the different critical temperatures extracted by DBHF or DB calculations depend on the different treatments of the nucleon self-energy [13].

In order to avoid complexity of the numerical techniques, the nuclear many-body effect can also be considered by a

density dependence in the couplings, which can parametrize the results of the DBHF in nuclear matter. Therefore the effective in-medium interaction and the nucleon self-energies are connected to the bare nucleon-nucleon interaction, which is determined further by  $NN$ -scattering data. As a result, the density dependent couplings induced in this way are completely independent of any phenomenological fit to data of the nuclear many-body effect, i.e., no free parameters are contained in the density dependent relativistic mean field (DRMF) theory. Along this line, the density dependence of the couplings have been proposed: parametrizations of the DBHF in nuclear matter in terms of relativistic mean field theory with scalar and vector nonlinear self-interaction were developed by Gmuca [14]. Similar approaches have been taken in [15,16], where they adjusted the density dependent couplings to reproduce numerically the nucleon self-energies resulting from the DBHF calculation. Recently, an analytical parametrization has been performed by Haddad and Weigel [17], who reproduced the DBHF nuclear matter results by using the parameter sets A, B, and C [18]. The analytical parametrization has also been applied to investigate Coulomb instability of highly excited nuclei [19], the

TABLE I. Parameter sets of Ref. [19] for the DRMF and Ref. [10] for the Walecka model used in the present work. We take the masses as:  $m_\sigma = 550$  MeV,  $m_\omega = 783$  MeV, and  $m_N = 939$  MeV. The saturation density is  $\rho_0 = 0.185, 0.174, 0.155,$  and  $0.148$  fm $^{-3}$  for the parameter set A, B, C, and the Walecka model, respectively.

Parameter sets	A	B	C	Walecka model
$g_\sigma^2(\rho_0)/4\pi$	6.7696	6.9342	7.271	9.7575
$a_{1,\sigma}$	1.2102	1.2705	1.3221	0
$a_{2,\sigma}$	1.6277	1.4683	1.4762	0
$g_\omega^2(\rho_0)/4\pi$	9.9278	10.3439	11.0055	15.15
$a_{1,\omega}$	1.2889	1.3764	1.4073	0
$a_{2,\omega}$	1.7771	1.6519	1.5778	0

additional rearrangement contributions [20], finite nuclei in Hartree approximation [21], and the nuclear deformation [22]. With the use of this analytical parametrization, we will extend the DRMF theory at zero temperature to the case of finite temperature and study the liquid-gas phase transition in warm nuclear matter.

The paper is organized as follows. In Sec. II, the equations of state for symmetric nuclear matter at finite temperature and density are presented. The results and discussion are given in Sec. III.

## II. NUCLEAR MATTER AT FINITE TEMPERATURE AND DENSITY

The Lagrangian density in the density dependent relativistic theory is given by [17]

$$\mathcal{L} = \bar{\psi}(i\gamma_\mu\partial^\mu - m_N + g_\sigma(\rho)\phi - g_\omega(\rho)\gamma_\mu\omega^\mu)\psi + \frac{1}{2}(\partial_\mu\phi\partial^\mu\phi - m_\sigma^2\phi^2) + \frac{1}{2}m_\omega^2\omega_\mu\omega^\mu - \frac{1}{4}F_{\mu\nu}F^{\mu\nu}, \quad (1)$$

where  $\phi$  is the  $\sigma$ -meson field,  $F_{\mu\nu} \equiv \partial_\mu\omega_\nu - \partial_\nu\omega_\mu$ , and  $\omega_\mu$  is for the  $\omega$ -meson field. We only consider the symmetric nuclear matter and do not include the  $\rho$ -meson effects. The couplings  $g_\sigma(\rho)$  and  $g_\omega(\rho)$  are taken to be the density dependence by [19]

$$\frac{g_i^2(\rho)}{g_i^2(\rho_0)} = 1 + a_{1,i}\left[1 - \left(\frac{\rho}{\rho_0}\right)^{1/3}\right] + a_{2,i}\left[1 - \left(\frac{\rho}{\rho_0}\right)^{1/3}\right]^2 \quad (i = \sigma, \omega), \quad (2)$$

where  $\rho_0$  is the saturation density of nuclear matter.

For symmetric nuclear matter, the equations of motion for the fields of nucleon and mesons can be obtained from Eq. (1) with mean field approximation (MFA):

$$\begin{aligned} \{\gamma_\mu(i\partial^\mu - \Sigma_{\text{tot}}^\mu) - [m_N - g_\sigma(\rho)\phi]\}\psi &= 0, \\ m_\sigma^2\phi &= g_\sigma(\rho)\langle\bar{\psi}\psi\rangle \equiv g_\sigma(\rho)\rho_s, \\ m_\omega^2\omega_0 &= g_\omega(\rho)\langle\psi^+\psi\rangle \equiv g_\omega(\rho)\rho, \end{aligned} \quad (3)$$

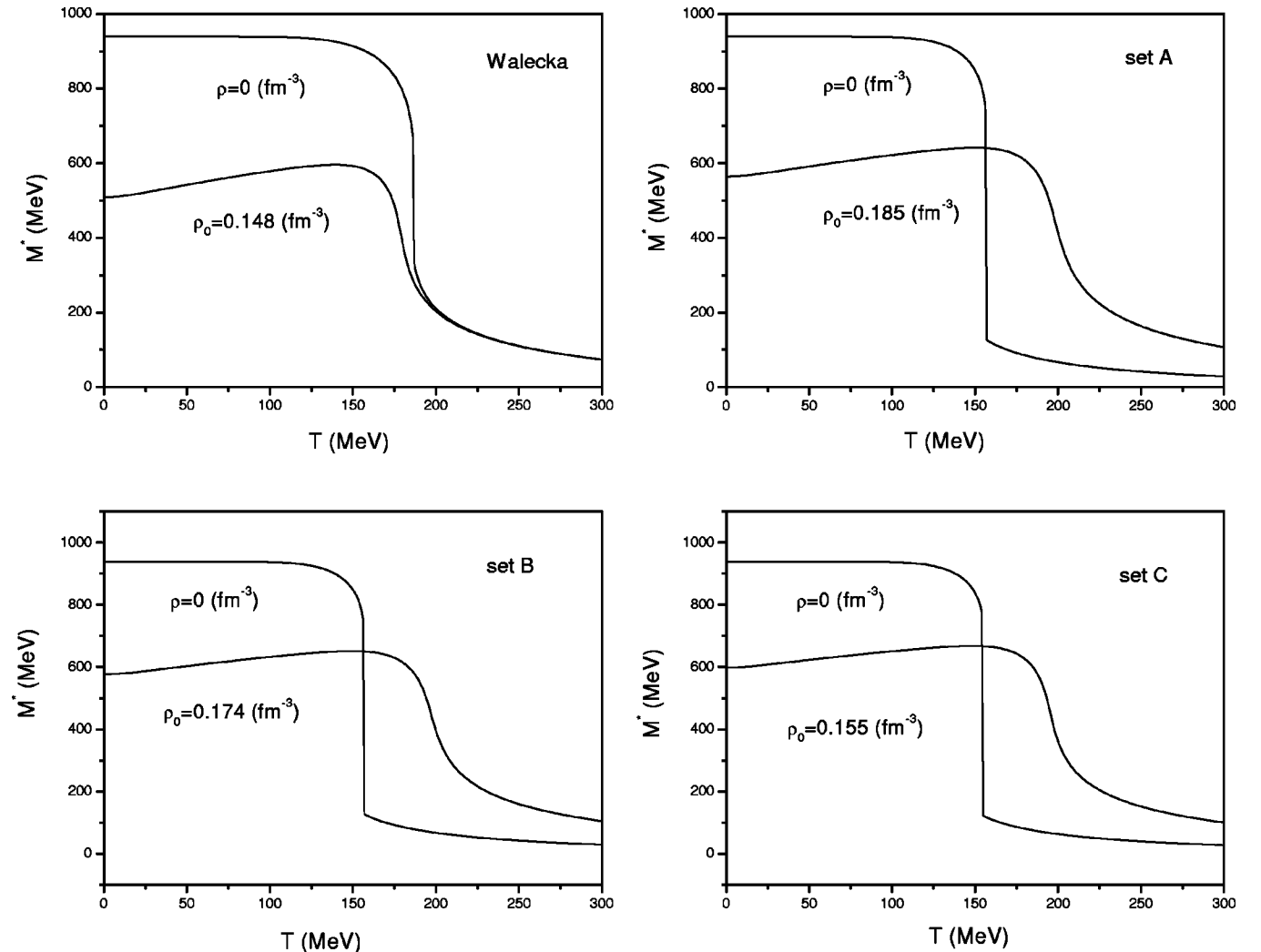


FIG. 1. Effective nucleon mass as a function of the temperature at zero and saturation densities.

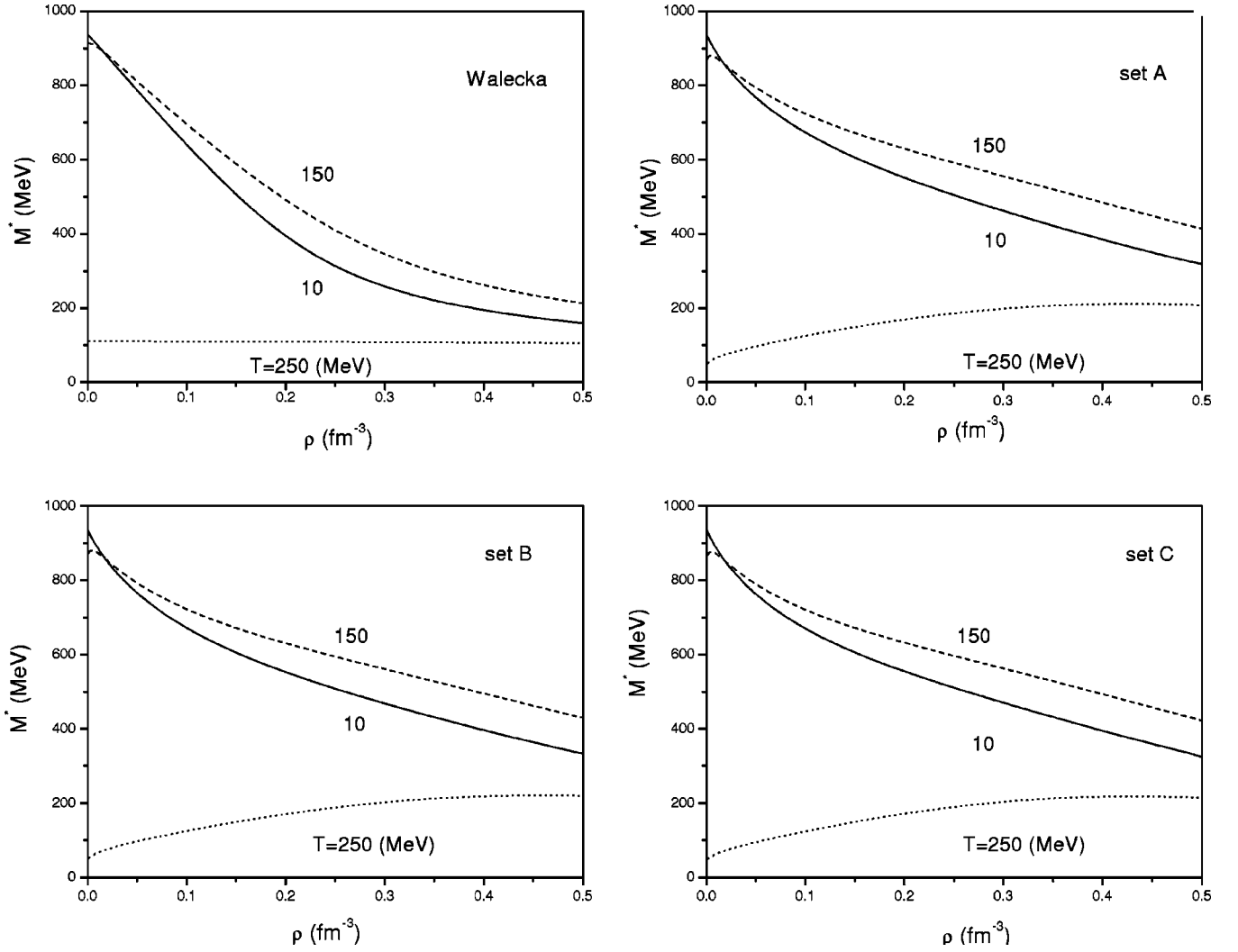


FIG. 2. Effective nucleon mass as a function of the baryon density at different temperatures.

where  $\langle \dots \rangle$  stands for the grand canonical ensemble expectation, and

$$\Sigma_{\text{tot}}^{\mu} = g_{\omega}(\rho) \omega^{\mu} + \Sigma_{\text{r}}^{\mu}, \quad (4)$$

is the vector self-energies with the rearrangement term given by

$$\Sigma_{\text{r}}^{\mu} = \left( \frac{\partial g_{\omega}(\rho)}{\partial \rho} \omega^{\nu} \langle \bar{\psi} \gamma_{\nu} \psi \rangle - \frac{\partial g_{\sigma}(\rho)}{\partial \rho} \phi \langle \bar{\psi} \psi \rangle \right) u^{\mu}, \quad (5)$$

which guarantees the thermodynamical consistency for the DRMF. Here  $u^{\mu} = (1, \vec{0})$  in the rest of frame and the rearrangement term in MFA can be expressed as

$$\Sigma_{\text{r}}^0 = \frac{\partial g_{\omega}(\rho)}{\partial \rho} \omega_0 \rho - \frac{\partial g_{\sigma}(\rho)}{\partial \rho} \phi \rho_s. \quad (6)$$

The equations of state for symmetric nuclear matter at finite temperature and density can be denoted as

$$\epsilon = 4 \int \frac{d^3 k}{(2\pi)^3} E^*(k) [n(k) + \bar{n}(k)] + \frac{1}{2} m_{\sigma}^2 \phi^2 + \frac{1}{2} m_{\omega}^2 \omega_0^2, \quad (7)$$

$$p = \frac{4}{3} \int \frac{d^3 k}{(2\pi)^3} \frac{k^2}{E^*(k)} (n(k) + \bar{n}(k)) - \frac{1}{2} m_{\sigma}^2 \phi^2 + \frac{1}{2} m_{\omega}^2 \omega_0^2 + \rho^2 \frac{\partial g_{\omega}(\rho)}{\partial \rho} \omega_0 - \rho \rho_s \frac{\partial g_{\sigma}(\rho)}{\partial \rho} \phi. \quad (8)$$

The second line in Eq. (8) stems from the rearrangement contribution [20]. Where  $E^* = \sqrt{k^2 + M^{*2}}$ , the effective nucleon mass is defined as  $M^* = m_N - g_{\sigma}(\rho) \phi$ .  $n(k)$  and  $\bar{n}(k)$  in Eqs. (7),(8) are the fermion and antifermion distribution functions

$$n(k) = \frac{1}{1 + \exp\{[E^*(k) - \nu]/T\}} \quad (9)$$

and

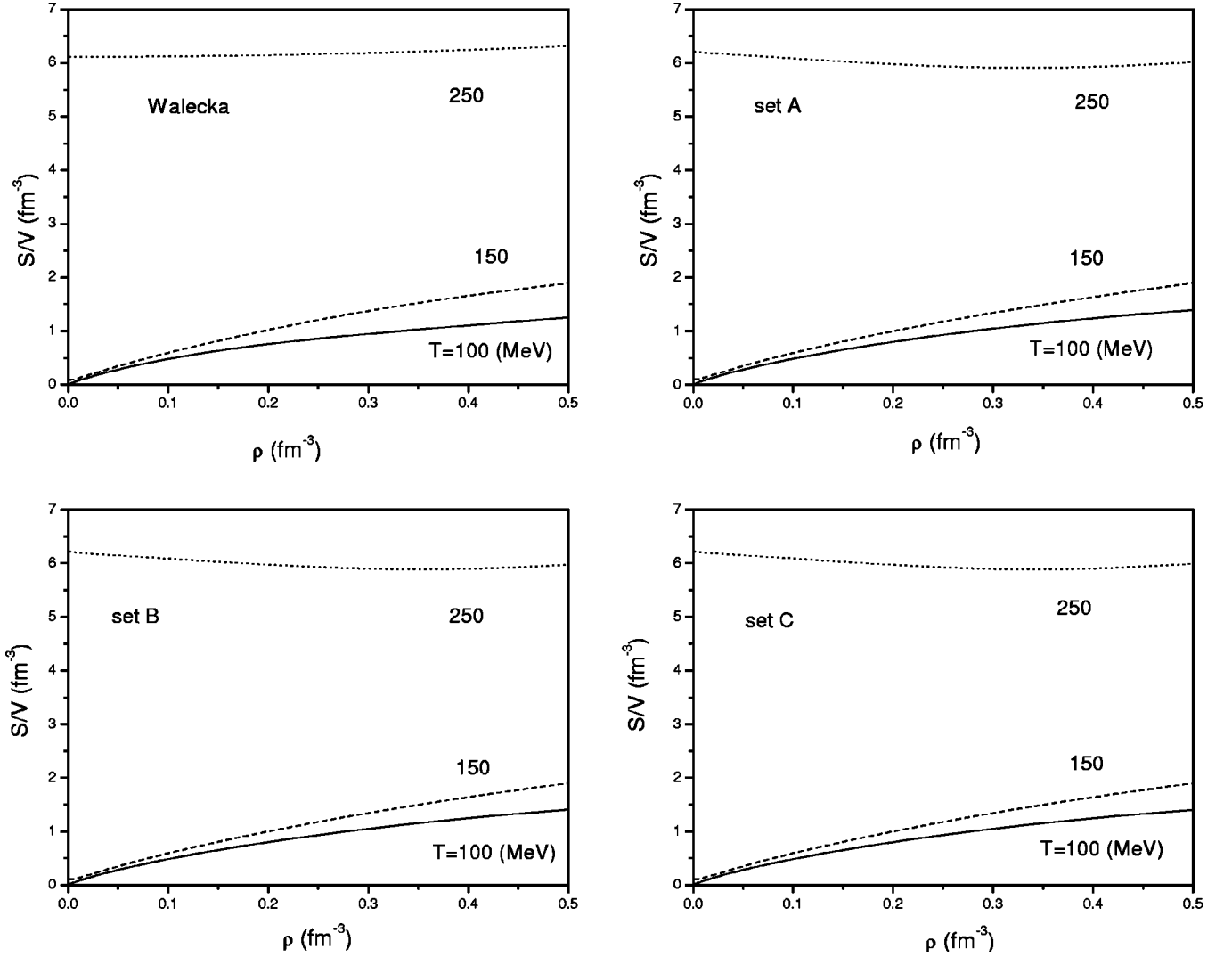


FIG. 3. Entropy density as a function of the baryon density at different temperatures.

$$\bar{n}(k) = \frac{1}{1 + \exp\{[E^*(k) + \nu]/T\}}, \quad (10)$$

where the effective chemical potential  $\nu$  is determined by the baryon density  $\rho$  as

$$\rho = 4 \int \frac{d^3k}{(2\pi)^3} [n(k) - \bar{n}(k)], \quad (11)$$

and the  $\nu$  is also related to the chemical potential  $\mu$  by the equation

$$\nu = \mu - g_\omega(\rho)\omega_0 - \Sigma_r^0. \quad (12)$$

The entropy density can be obtained as

$$s = \frac{1}{T} \left\{ m_\omega^2 \omega_0^2 + 4 \int \frac{d^3k}{(2\pi)^3} E^*(k) [n(k) + \bar{n}(k)] \right. \\ \left. + \frac{4}{3} \int \frac{d^3k}{(2\pi)^3} \frac{k^2}{E^*(k)} [n(k) + \bar{n}(k)] \right\} + \frac{1}{T} \left[ \rho^2 \frac{\partial g_\omega(\rho)}{\partial \rho} \omega_0 \right. \\ \left. - \rho \rho_s \frac{\partial g_\sigma(\rho)}{\partial \rho} \right] - \frac{\mu \rho}{T}. \quad (13)$$

Thus, the energy density, the pressure, and the entropy density for symmetric nuclear matter at finite temperature and finite density can be calculated self-consistently by Eqs. (7), (8), and (13).

### III. RESULTS AND DISCUSSION

In our calculations, we take the parameters of Ref. [19] for the DRMF, which are given in Table I. In order to make the comparison, we also use density independent parameters of Ref. [10] for the Walecka model.

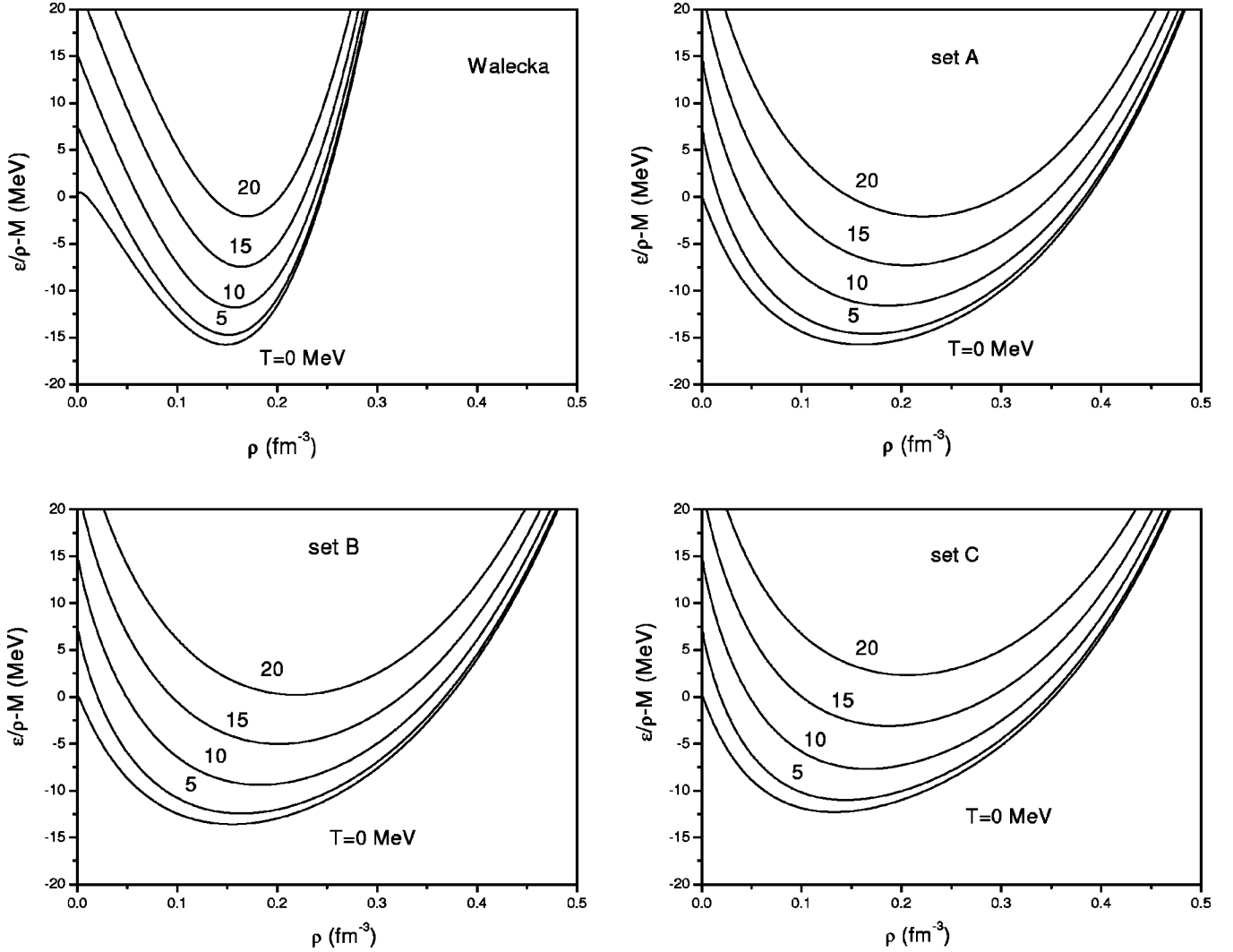


FIG. 4. Energy per nucleon as a function of the baryon density at different temperatures.

Figure 1 shows the effective nucleon mass  $M^*$  as a function of temperature  $T$  at zero and saturation densities. At zero density, the results of the DRMF and the Walecka model coincide basically in the lower-temperature region, and separate clearly in the regions of high temperature. The results show that a first-order phase transition appears at  $\rho=0$ ,  $T \approx 160$  MeV for the DRMF with parameter sets A, B, and C, and  $T \approx 185$  MeV [23] for the Walecka model. The result shows that the attraction between nucleons is so strong in both DRMF and Walecka model that the nucleon-antinucleon pairs can be formed at high temperature, and leads to an abrupt change of  $M^*$  in the regions of high temperature. The mechanism of this first-order phase transition is not clear. Due to the big change of  $M^*$  that took place in the regions of high temperature for both the DRMF and the Walecka model, this first-order phase transition might be related to the formation of new matter.

At saturation density (note that different parameter sets in the DRMF have different saturation densities [19]) the effective nucleon mass increases slowly in the regions of lower temperature, and then decreases in the regions of higher temperature. In comparison with the Walecka model, the curves

with the parameter sets A, B, and C in the DRMF are quite similar in shape at zero or saturation density, as mentioned in Ref. [21], and the three parameter sets A, B, and C differ only in different tensor forces, which cannot give a large influence on the effective nucleon mass.

We show the behavior of the effective nucleon mass as a function of baryon density at different temperatures for both the DRMF and the Walecka model in Fig. 2. We also calculate the effective nucleon mass at zero temperature, but we find that the results are quite similar to those obtained at  $T = 10$  MeV. As shown for the Walecka model, the large gap of  $M^*$  between the low and high temperatures also appears for the DRMF. The effective nucleon mass in the DRMF at  $T = 250$  MeV first increases and then decreases slowly. This result is different from that in the Walecka model. It can be seen from Fig. 2 that the effect of temperature on the effective nucleon mass in the DRMF is considerable in contrast to the Walecka model.

We calculate the entropy density as a function of the density at different temperatures. The results are presented in Fig. 3. For high temperature ( $T = 250$  MeV), it has been shown that there is a large gap between  $T = 150$  and 250

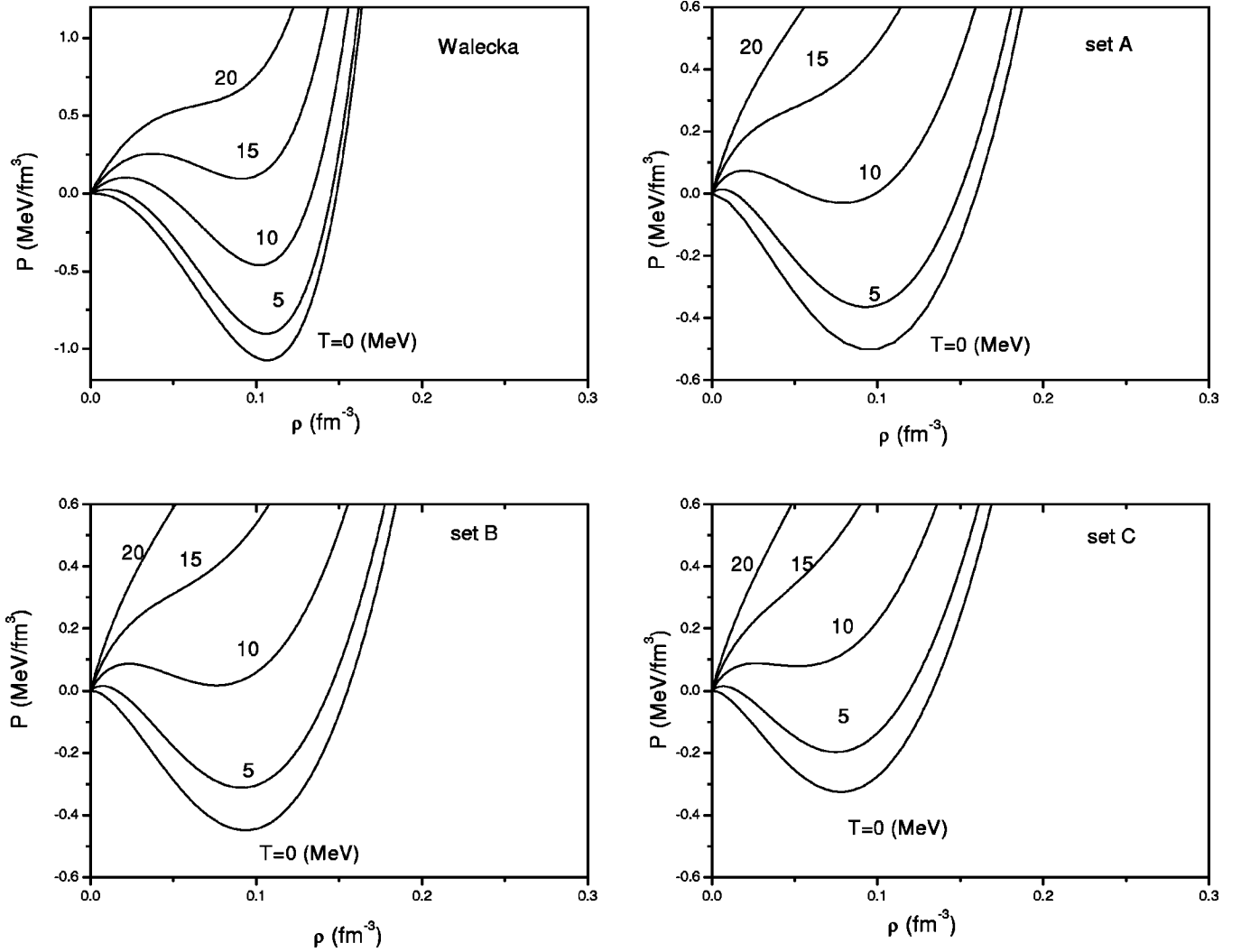


FIG. 5. Pressure as a function of the baryon density at different temperatures.

MeV in the entropy density with the increasing density for all the models. This large gap appears even at zero density, and illustrates that the behavior of the entropy density in the high-temperature regions is consistent with the decrease of  $M^*$  at zero density as shown in Fig. 2, and resembles a phase transition.

Figure 4 shows the energy per nucleon as a function of the baryon density at different temperatures. With the increasing temperature, nuclear matter becomes less bound and the saturation curves in the DRMF are flatter than those in the Walecka model. These results mean that the equation of state (EOS) of nuclear matter in the DRMF is softer compared to that obtained in the Walecka model.

We present the pressure of nuclear matter as a function of baryon density at different temperatures in Fig. 5. Because the value of incompressibility  $K$  is proportional to  $\partial p/\partial \rho$  (calculated at the equilibrium point where the pressure vanishes), so  $K$  decreases with the increasing temperature, and among the different parameter sets in the DRMF, the parameter set C always gives the softer EOS for a fixed temperature. Therefore we can conclude that the incompressibility of nuclear matter decreases with the increasing temperature.

The curves of the pressure exhibit a typical Van der Waals-like interaction where liquid and gaseous phases coexist. For very low density the pressure increases with increasing temperature just as happens in an ideal gas. It decreases subsequently due to the attractive interaction of the  $\sigma$ -meson field, and finally increases as a result of the repulsion from the  $\omega$ -meson field. When the temperature increases, the local minimum in the pressure is less pronounced and disappears when the temperature is equal to the critical values  $T_c$ , which is determined by  $\partial p/\partial \rho|_{T_c} = \partial^2 p/\partial \rho^2|_{T_c} = 0$ . In com-

TABLE II. Values for the critical temperature  $T_c$  and the effective nucleon mass  $M_c^*$  in MeV, critical density  $\rho_c$  in  $\text{fm}^{-3}$ , and the pressure  $p_c$  in  $\text{MeV}/\text{fm}^3$ .

	$T_c$	$\rho_c$	$p_c$	$M_c^*$
Walecka model	18.30	0.0650	0.430	760
A	12.66	0.0475	0.152	775
B	12.00	0.0483	0.151	771
C	10.5	0.0393	0.103	789

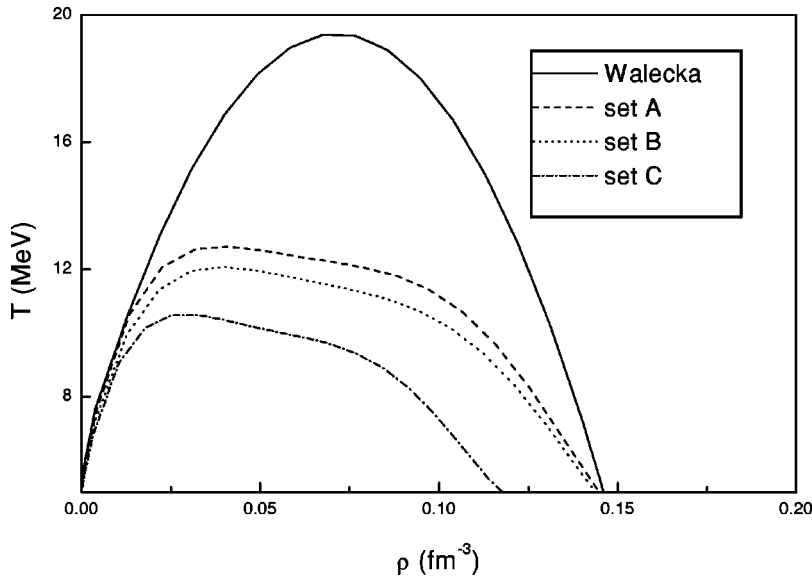


FIG. 6. Temperature as a function of the baryon density (phase diagram).

parison with the Walecka model in Fig. 5 the  $p$ - $\rho$  isotherms in the DRMF have a shallower and flatter valley than those in the Walecka model. The calculated critical values of temperature, density, pressure, and effective nucleon mass by the DRMF and the Walecka model are given in Table II. The critical temperature given by the DRMF with the parameter set A is  $T_c = 12.66$  MeV which is quite close to the recent experimental value  $T_c = 13.1 \pm 0.6$  MeV [7]. The critical temperatures  $T_c = 12.0$  and 10.5 MeV are given by the parameter set B and C, respectively.

In Fig. 6 we show the phase diagram given by the DRMF and Walecka model. The phase coexistence boundary is determined when the liquid and gas phases satisfy the following equilibrium conditions:  $T_{\text{liquid}} = T_{\text{gas}}$ ,  $\mu_{\text{liquid}} = \mu_{\text{gas}}$ , and  $p_{\text{liquid}} = p_{\text{gas}}$ . The area below the coexistence curve is a region for the mixture of gas and liquid, while the region over the coexistence curve is that for uniform nuclear matter. It can be seen that the coexistence region given by the DRMF is smaller than that given by the Walecka model.

In summary, we have investigated the thermodynamical properties of nuclear matter in the DRMF and the Walecka

model, and presented how the effective nucleon mass, energy per nucleon, pressure, and entropy density behave as a function of the density for various temperatures. At zero density we find that the DRMF model exhibits a phase transition at  $T \approx 160$  MeV just as in the Walecka model at  $T \approx 185$  MeV. We have also studied the liquid-gas phase transition and obtained a smaller phase coexistence region by the DRMF model. The critical temperature given by the DRMF with the parameter set A is  $T_c = 12.66$  MeV which is consistent with the recent experimental findings  $T_c = 13.1 \pm 0.6$  MeV [7]. The first-order liquid-gas phase transition which may take place in the warm and dilute matter produced in heavy-ion reactions is one of interesting problems in nuclear physics. The search for signals of the liquid-gas nuclear phase transition experimentally and the theoretical study of the transition mechanism are still expected.

#### ACKNOWLEDGMENTS

This project was supported in part by major state basic research developing program with No. G2000077400 and National Science Foundation of China.

- 
- [1] J. E. Finn *et al.*, Phys. Rev. Lett. **49**, 1321 (1982); M. Mahi *et al.*, *ibid.* **60**, 1936 (1988); M. L. Gilkes *et al.*, *ibid.* **73**, 1590 (1994).
  - [2] W. A. Kupper, G. Wegmann, and E. R. Hilf, Ann. Phys. (N.Y.) **88**, 454 (1974).
  - [3] B. Friedman and V. R. Pandharipande, Nucl. Phys. **A361**, 502 (1981).
  - [4] H. Jaqaman, A. Z. Mekjian, and L. Zamick, Phys. Rev. C **27**, 2782 (1983).
  - [5] D. Bandyopadhyay, C. Samanta, S. K. Samaddar, and J. N. De, Nucl. Phys. **A511**, 1 (1990).
  - [6] G. Brown, H. Bethe, and G. Baym, Nucl. Phys. **A375**, 481 (1982).
  - [7] T. Li *et al.*, Phys. Rev. C **49**, 1630 (1994).
  - [8] B. D. Serot and J. D. Walecka, Adv. Nucl. Phys. **16**, 1 (1986); Int. J. Mod. Phys. E **6**, 515 (1997).
  - [9] R. J. Furnstahl and B. D. Serot, Phys. Rev. C **55**, 1499 (1997).
  - [10] M. Malheiro, A. Delfino, and C. T. Coelho, Phys. Rev. C **58**, 426 (1998).
  - [11] B. ter Haar and R. Malfliet, Phys. Rep. **149**, 207 (1987); Phys. Rev. Lett. **59**, 1652 (1987).
  - [12] M. Baldo, *et al.*, Nucl. Phys. **A583**, 599c (1995).
  - [13] H. Huber, F. Weber, and M. K. Weigel, nucl-th/9803026, 1998.
  - [14] S. Gmuca, J. Phys. G **17**, 1115 (1991); Z. Phys. A **342**, 387 (1992).
  - [15] R. Brockmann and H. Toki, Phys. Rev. Lett. **68**, 3408 (1992).
  - [16] H. L. Shi, B. Q. Chen, and Z. Y. Ma, Phys. Rev. C **52**, 144

- (1995).
- [17] S. Haddad and M. K. Weigel, Phys. Rev. C **48**, 2740 (1993).
- [18] R. Brockman and R. Machleidt, Phys. Rev. C **42**, 1965 (1990).
- [19] S. Haddad and M. K. Weigel, Phys. Rev. C **49**, 3228 (1994).
- [20] C. Fuchs, H. Lenske, and H. H. Wolter, Phys. Rev. C **52**, 3043 (1995).
- [21] F. Ineichen, M. K. Weigel, and D. von-Eiff, Phys. Rev. C **53**, 2158 (1996).
- [22] M. L. Cescato and P. Ring, Phys. Rev. C **57**, 134 (1998).
- [23] J. Theis, H. Stöcker, and J. Polony, Phys. Rev. D **28**, 2286 (1983).